Organic LETTERS

Letter

pubs.acs.org/OrgLett

Triple Boron-Cored Chromophores Bearing Discotic 5,11,17-Triazatrinaphthylene-Based Ligands

Feng Qiu,[†,‡] Fan Zhang,[*,‡] Ruizhi Tang,[‡] Yubin Fu,[§] Xinyang Wang,[‡] Sheng Han,[†] Xiaodong Zhuang,[‡] and Xinliang Feng[‡,§]

[†]School of Chemical and Environmental Engineering, Shanghai Institute of Technology, Shanghai 201418, P. R. China

[‡]School of Chemistry and Chemical Engineering, State Key Laboratory of Metal Matrix Composites, Shanghai Jiao Tong University, Shanghai 200240, P. R. China

[§]Department of Chemistry and Food Chemistry & Center for Advancing Electronics Dresden (cfaed), Technische Universitaet Dresden, Dresden, Germany

Supporting Information

ABSTRACT: A series of novel chromophores fused with multiple boron cores have been successfully synthesized by the complexation of three difluoroboryl or diphenylboryl at the periphery of 5,11,17-triazatrinaphthylene derivative ligands. Their sterically congested molecular scaffolds with expanded π-conjugated discotic backbones render them with unique electronic properties including large Stokes shifts, tunable electrochemical behaviors, and low-lying LUMO energy levels up to −3.18 eV.

Owing to their rich optoelectronic properties and excellent self-assembly behavior on the surface, fluorescent dyes hold great promise in a wide scope of applications such as nanomaterials, organic semiconductors, and biological probes.[1] Among them, boron dipyrromethene (BODIPY, **I**), comprising a four-coordinated boron center chelated by bidentate heterocyclic ligand and two fluorine atoms (Scheme 1), exhibits rich photophysical properties, including high absorption coefficients, moderate fluorescence quantum yields, which has been widely utilized in organic solar cells, organic light-emitting diodes, sensing, imaging, etc.[2] Unfortunately, BODIPY dye always suffers from some shortcomings, such as small Stokes shift, low photostability, and poor emission in solid state.[3] Thus, development of new boron-cored dyes with rich optoelectronic properties, which have adjustable emitting behavior, good fluorescence quantum yield, high charge carrier mobility, etc., are highly desirable.

Scheme 1. Typical Boron-Cored Chromophores

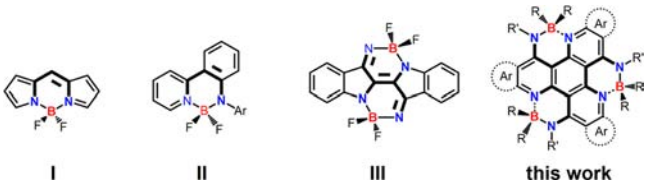

Recently, constructing boron-containing chromophores through the incorporation of four-coordinated boron-cored segment into various bidentate aromatic skeletons have made significant progress.[4] For example, the anilido-pyridine boron difluoride dyes (**II**) exhibit exceptional photostability and large Stokes shifts as a result of their desymmetric skeleton with donor−acceptor structures.[5] The dual-boron-cored chromophores with multiple functions including near-infrared spectroscopic properties (**III**),[6] aggregation-induced emission activity,[4c] or reversible piezochromism[7] have also been achieved. Obviously, in these molecules, the four-coordinated boron-cored unit comprising a weak B,N-coordinated bond and a strong B,N-covalent bond not only possesses a shape-persistent skeleton but also plays a crucial role in tuning the solid-state packing and optoelectronic properties.[8] Furthermore, the number and position of the four-coordinated boron center in expanded π-conjugated system also has strong influence on its electronic and geometric structures.[9] Despite the remarkable achievements in the synthesis of triple symmetric heterocoronenes with different heteroatoms (e.g., 1,5,9-triazacoronenes, trichalcogenasumanene, etc.),[10] to the best of our knowledge, the heterocoronenes fused with multiple four-coordinated boron units is still rarely documented, mainly due to the lack of the multidentate aromatic ligands capable for chelating several boron atoms in one system.

In this work, we present the synthesis of a series of novel chromophores fused with triple boron cores by the complexation of boron atoms with 6,12,18-tris(alkyl amine)-5,11,17-triazatrinaphthylene derivatives as the ligands. These new chromophores were fully characterized by X-ray single crystal analyses, optical spectroscopy, and cyclic voltammogram, and their geometric and electronic structures can be effectively tuned through changing the substituents around the boron cores.

Received: February 1, 2016
Published: March 10, 2016

DOI: 10.1021/acs.orglett.6b00335
Org. Lett. 2016, 18, 1398−1401

The synthetic route toward triple boron-cored chromophores is shown in Scheme 2. The key intermediate of 6,12,18-trichloro-

Scheme 2. Synthesis of Triple Boron-Cored Chromophores

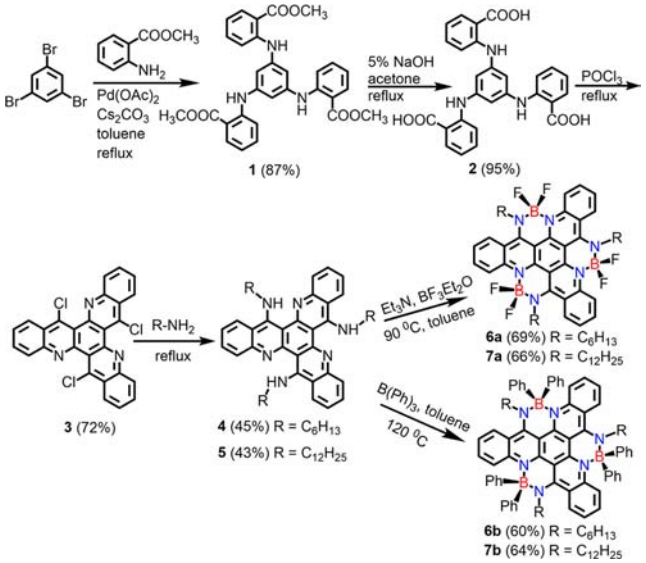

5,11,17-triazatrinaphthylene (**3**) was prepared from 1,3,5-tribromobenzene by using a three-step sequence of Buchwald–Hartwig coupling, hydrolysis, and dehydration cyclization, in the yield of 87%, 95%, and 72%, respectively.[11] Then the heterocyclic ligands with anilido-pyridine structure, 6,12,18-tris(hexylamine)-5,11,17-triazatrinaphthylene **4** and 6,12,18-tris(dodecylamine)-5,11,17-triazatrinaphthylene **5**, were obtained as yellow solid powder with the yields of 45% and 43%, respectively, by the coupling of compound **3** with the different alkylamines upon heating to 135 °C in solvent-free conditions. After the treatment of ligand **4** or **5** with excess amount of boron trifluoride etherate ($BF_3{\cdot}OEt_2$ 3.0 equiv) using triethylamine as catalyst in toluene at 80 °C for 24 h, **6a** or **7a** was obtained as yellow solid in a yield of 69% or 66%, respectively, after purified by silica gel column chromatography. Replacing $BF_3{\cdot}OEt_2$ with triphenylboron under the similar reaction conditions, compound **6b** or **7b** was achieved in the yield of 60% or 64%, respectively. All compounds **6a,b** and **7a,b** were fully characterized by ^1H, ^{13}C, and ^{11}B NMR spectroscopies as well as high-resolution mass spectrometry. As an example, the proton signal of the secondary amine groups in ligand **4** at around 14.6 ppm in ^1H NMR spectrum (Figure S18) disappeared, after ligated with boron atom to form compound **6a**. Moreover, the proton peaks of the aromatic skeleton in **6a** are significantly shifted to the low field in comparison with those of the dissociated ligand **4**, resulting from the electron deficient nature of BF2 moiety.[4d,9a] In ^{11}B NMR spectra of **6a,b** or **7a,b**, only one boron signal can be observed, indicative of the same chemical environment for the three boron atoms of each compound. All compounds exhibit good solubility in common organic solvents, and high stability both in solid state and solution without any observed decomposition when exposed in the air for several months.

Single crystals of **6a** and **6b** were obtained at ambient temperature by slowly diffusing methanol into its acetone and toluene solutions, respectively (Figure 1). From the top view in Figure 1a, the main backbones of both **6a** and **6b** exhibit a disc-shape skeleton, consisting of ten fused six-membered rings. In their side views (Figure S2), the slight deformation of the main

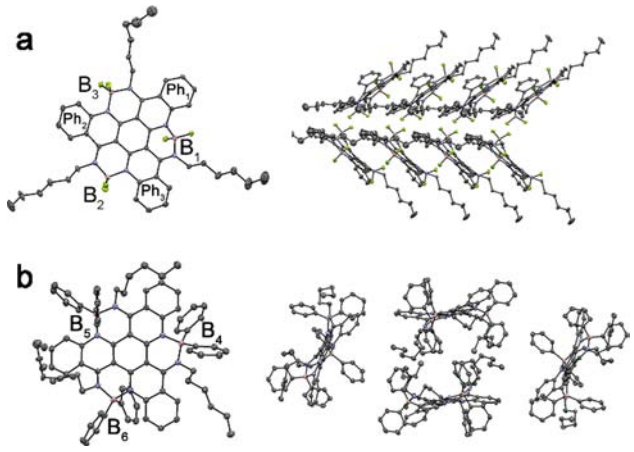

Figure 1. Crystal structures of **6a** (a) and **6b** (b) (top views and packing diagrams).

backbones can be observed. For compound **6a**, the three benzene rings on the peripheries of the main backbone bend to the same direction, yielding a torsion angle of 18.76° (Ph_1), 10.69° (Ph_2), and 25.08° (Ph_3), respectively, with respect to the central benzene ring. Each boron atom bearing two fluorine atoms is chelated by the two nitrogen atoms of ligand **4** to form a pseudo tetrahedron geometry around the boron center. These boron atoms are deviated from the mean plane of the central benzene ring with the dihedral angles of 54.59° (B_1), 12.72° (B_2), and 5.37° (B_3), respectively. Such twisted conformation can be attributed to the formation of a relatively crowed circumstance upon the fusion of three BF_2 units with ligand **4** through three anilido-pyridine bidentates.[5] By contrast, attaching two bulky phenyl substituents on each boron atom in **6b** creates a more congested conformation, thus leading to a much strongly deformed molecular skeleton. Accordingly, the plane comprising one boron atom and the two chelated nitrogen atoms form a larger dihedral angle of 15.33° (B_4), 25.01° (B_5), and 21.09° (B_6), relative to the central benzene ring, respectively.[8b] Notably, there is only slight difference between the coordination and covalent B–N bonds lengths (1.53 and 1.56 Å for **6a**; 1.56 and 1.61 Å for **6b**), suggesting that electrons are likely well delocalized in each N–B–N segment of the as-prepared chromophores.[4d,9c] In the packing diagram, compound **6a** exhibits a herringbone packing motif consisting of the slipped stacking columns. Each column is tilted at an angle of 58.97° with respect to its neighboring column. The distance between the two neighboring π-stacked molecules is 3.60 Å.[12] Additionally, such close-packed structures are enforced through the edge-to-face C–H$\cdots\pi$ interactions (2.68 Å) between the methylene group and adjacent fused backbone.[4c] Therefore, compound **6a** possesses a compact packing structure in solid state. In contrast, there is no distinct intermolecular π–π stacking interaction observed in the packing diagram of **6b**, which can be attributed to the shielding effect of the bulky phenyl substituents on boron atoms. The main fused backbones of the neighboring molecules are arranged in edge-to-edge fashions with the distance from 3.55 to 3.98 Å, and certain C–H$\cdots\pi$ interactions (~3.94 Å) between the neighboring molecules can be identified.

The optical properties of **6a,b** and **7a,b** in dichloromethane were investigated by means of ultraviolet–visible (UV–vis) and photoluminescence (PL) spectroscopy. In the UV–vis spectra (Figure 2a), compound **6a** shows a set of absorption bands appearing at around 284 and 368 nm, as well as two shoulder

DOI: 10.1021/acs.orglett.6b00335
Org. Lett. 2016, 18, 1398–1401

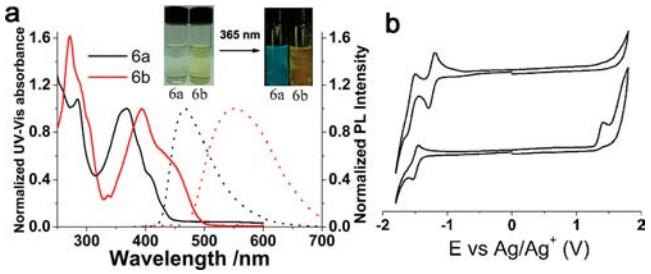

Figure 2. (a) UV−vis absorption and PL spectra of **6a**,**b**, respectively (Inset: digital images of **6a**,**b** under sunlight and UV light (1.0×10^{-6} M in CH_2Cl_2). (b) Cyclic voltammograms of **6a**,**b** at a scan rate of 100 mV/s (in CH_2Cl_2, 0.1 mol/L n-Bu_4NPF_6).

peaks at 391 and 412 nm, respectively. Such broad featureless absorption bands reveal the less rigid molecular structures, in line with the crystallographic analyses above.[13] The absorption maxima at 368 typically originates from the $\pi-\pi^*$ transitions of the aromatic backbone, which shows a moderate bathochromic shift (16 nm) with respect to ligand **4** (Figure S5), suggesting the extended π-conjugation for **6a**. In addition, the weak shoulder peak at 412 nm can be assigned to the intramolecular charge transfer (ICT) indicated by the solvatochromic effect in solution (Figure S6).[4d,5] These blue shifts of the main absorption bands with increasing the polarity of solvents suggest that the compound **6a** could be facile to be polarized at ground state. This result is also in agreement with that of time-dependent density functional theory (TD-DFT) calculation in which the ICT peak at 412 nm governs the electron transition from the highest occupied molecular orbital (HOMO) to the lowest unoccupied molecular orbital (LUMO) (Figure S10). Interestingly, the absorption maxima at λ_{max} = 454 nm for **6b** is remarkably red-shifted by 26 nm by comparison to that of **6a**, manifesting that the substituents on the boron centers have large influence on their optical properties.[9b,14] Such phenomenon can be ascribed to that the stronger electron-donating effect of phenyl groups for **6b** as compared with that of fluorine atoms in **6a** enables to arise the HOMO energy level efficiently through adjusting the substituent in boron center. For **7a** and **7b**, the UV−vis absorption profiles are similar to those of compound **6a** and **6b**, respectively (Figure S7). The spin-coated films of these compounds exhibit broad absorption maxima with bathochromic shifts (4 nm for **6a**, 5 nm for **6b**), revealing the strengthened intermolecular interactions in solid state (Figure S8).[10b,13]

No emission can be observed for the ligands **4** and **5** either in solution or solid states, which is a normal phenomenon for nitrogen-containing chromophores due to the strong photo induced electron transfer (PET) effect.[15] After incorporation of BF_2 moieties with **4**, **6a** shows blue luminescence with emission maxima (λ_{em}) at 474 nm, while the λ_{em} of **6b** is bathochromically shifted by 93 nm with orange emission (Figure 2a). Such luminescent behavior for **6a** or **6b** is probably attributed to the confinement of the nitrogen lone-pair electrons through the formation of the B−N coordinated bond to avoid PET effect. Unlike other rigid 3-fold symmetric polycyclic aromatic hydrocarbons (PAHs), the emission profiles of compounds **6a** and **6b** are not the mirror image of their absorption profiles, manifesting their deformed structures in the excited states.[5] Moreover, compounds **6a** and **6b** exhibit large Stokes shifts of 106 and 157 nm, respectively, which are among the highest values of the B,N-containing chromophores.[16] Such results are reasonably attributed to the asymmetric structures of these molecules associated with their deformed discotic main backbones as the consequence of the congested circumstances,[4c] which is consistent with their single crystal structure analyses. The fluorescence quantum yields of the as-prepared molecules (from 2.46% to 1.91%) are much lower than those of the anilido-pyridine boron-core compounds, presumably attributable to the enhanced nonradiative deactivation from the multisubstituents of boron units and the relatively deformable molecular main backbones.[5,16a] Fluorescence lifetime values of **6b** and **7b** (3.20 and 3.15 ns, respectively) are approximately two times larger than those of **6a** and **7a** (1.73 and 1.60 ns, respectively) (Table 1), probably stemming from the weakened polarity of the phenyl

Table 1. Absorption, Fluorescence, and Photophysical Data of Triple Boron-Cored Chromophores in CH_2Cl_2

	λ_{abs}[a] (nm)	ε_{max} (m^{-1} cm^{-1})	λ_{em}[b] (nm)	Φ_f[c]	SS[c] (nm)	τ_f (ns)
6a	368	10745	474	2.46	106	1.73
6b	394	10317	551	1.97	157	3.20
7a	368	9768	474	2.22	106	1.60
7b	394	9687	551	1.91	157	3.15

[a]Longest absorption maximum. [b]Emission maximum upon excitation at the longest absorption maximum. [c]Absolute quantum yield.

substituents compared with the fluorine groups around the boron cores. However, the more congested molecular conformation for **6b** or **7b** might constrain the conformation change, which might be also beneficial to the elongation of the fluorescence lifetime.[17]

The electronic structures of the as-prepared molecules were further evaluated using cyclic voltammetry (CV) in CH_2Cl_2 (Figure 2b, Table S1). Compound **6a** exhibits two successive one-electron reduction processes with the redox peaks at E_{red}^1 = −1.17 V and E_{red}^2 = −1.51 V, respectively, and no oxidation process was observed within the range of chemical window under the experimental conditions. Such successive reduction process indicates that the skeleton of **6a** has the extended π-conjugated system, and the electron can be effectively delocalized over the whole molecular backbone. Accordingly, the LUMO energy level of **6a** was derived to be −3.17 eV based on the onset value of the first reduction potential. The HOMO energy level of −5.97 eV was calculated on the basis of the optical band gap (2.80 eV) and the LUMO value. This result demonstrates that compound **6a** shows the typical electron-deficient character, which might serve as n-type material in organic electronics.[18] Differently, compound **6b** gives only one one-electron reduction process with an E_{red}^1 of −1.41 V, as well as one irreversible oxidation peak at E_{ox}^1 = 1.31 V. Accordingly, the LUMO and HOMO energy levels of **6b** are −2.93 and −5.36 eV, respectively. Such different electrochemical behavior between the two molecules suggests that the substituted groups attached to the boron atoms on the molecular periphery of **6a** or **6b** enable strongly affecting their electronic structures and thus tune the optical properties of these triple boron-cored molecules. As expected, the CV profiles of **7a** and **7b** are also similar to those of **6a** and **6b**, respectively (Figure S12). In order to gain further insight into the electronic structures of these new boron-cored chromophores, theoretical calculations based on time-dependent density functional theory (TD-DFT) (RB3LYP/6-31G (d) level) have been performed (Figure S11, Table S1). For all compounds, both the HOMO and the LUMO energy levels are predominantly localized on the discotic backbones, indicative of their extended π-conjugated

DOI: 10.1021/acs.orglett.6b00335
Org. Lett. 2016, 18, 1398−1401

systems. However, the distribution of these frontier orbitals over the whole conjugated backbone are not uniform, especially for **6b**. Such phenomena could be rationally attributed to the less planarity of the discotic backbones caused by the crowded molecular circumstances, as shown in their crystal structure aforementioned. The computational HOMO energy levels of −6.14 and −5.62 eV for **6a** and **6b** also well coincide with that of experimental results.

In summary, we demonstrate an efficient synthesis of a new family of triple boron-cored chromophores by the coupling of three boron atoms with multidentate 5,11,17-triazatrinaphthylene derivative ligands. The structural analyses and optoelectronic measurements revealed that the fusion of the multiple boron moieties in the molecular main backbones of such kinds of chromophores not only created the extended π-conjugated system, but also led to the relatively deformable fused backbones with respect to the sterically congested molecular conformations. Their unique geometric structures render them with the very rich optoelectronic properties, including large Stokes shifts, relatively low-lying LUMO energy levels, and tunable electrochemical behaviors through the substituents on boron atoms. Therefore, they may serve as promising candidates applicable for electronic devices and photo- or electrochemical-stimulated catalysis.

■ ASSOCIATED CONTENT

Supporting Information

The Supporting Information is available free of charge on the ACS Publications website at DOI: 10.1021/acs.orglett.6b00335.

Experimental details, NMR spectra, UV−vis spectra, PL spectra, TGA data, and cyclic voltammetry (PDF)
Single-crystal X-ray diffraction data for **6a** (CIF)
Single-crystal X-ray diffraction data for **6b** (CIF)

■ AUTHOR INFORMATION

Corresponding Author

*E-mail: fan-zhang@sjtu.edu.cn.

Notes

The authors declare no competing financial interest.

■ ACKNOWLEDGMENTS

This work was financially supported by the National Basic Research Program of China (973 Program: 2013CBA01602 and 2012CB933404), the National Natural Science Foundation of China (21574080, 21102091, and 21504057), and the Shanghai Committee of Science and Technology (15JC1490500). We also thank Merck KGaA for financial support.

■ REFERENCES

(1) (a) Weiss, S. *Science* **1999**, *283*, 1676−1683. (b) An, B.-K.; Gihm, S. H.; Chung, J. W.; Park, C. R.; Kwon, S.-K.; Park, S. Y. *J. Am. Chem. Soc.* **2009**, *131*, 3950−3957. (c) Mishra, A.; Fischer, M. K. R.; Bäuerle, P. *Angew. Chem., Int. Ed.* **2009**, *48*, 2474−2499. (d) Liu, H.; Xu, J.; Li, Y.; Li, Y. *Acc. Chem. Res.* **2010**, *43*, 1496−1508.

(2) (a) Loudet, A.; Burgess, K. *Chem. Rev.* **2007**, *107*, 4891−4932. (b) Ulrich, G.; Ziessel, R.; Harriman, A. *Angew. Chem., Int. Ed.* **2008**, *47*, 1184−1201.

(3) Frath, D.; Massue, J.; Ulrich, G.; Ziessel, R. *Angew. Chem., Int. Ed.* **2014**, *53*, 2290−2310.

(4) (a) Li, D.; Zhang, H.; Wang, Y. *Chem. Soc. Rev.* **2013**, *42*, 8416−8433. (b) Galer, P.; Korošec, R. C.; Vidmar, M.; Šket, B. *J. Am. Chem. Soc.* **2014**, *136*, 7383−7394. (c) Fu, Y.; Qiu, F.; Zhang, F.; Mai, Y.; Wang, Y.; Fu, S.; Tang, R.; Zhuang, X.; Feng, X. *Chem. Commun.* **2015**, *51*, 5298−5301. (d) Sun, L.; Zhang, F.; Wang, X.; Qiu, F.; Xue, M.; Tregnago, G.; Cacialli, F.; Osella, S.; Beljonne, D.; Feng, X. *Chem. - Asian J.* **2015**, *10*, 709−714. (e) Cheng, X.; Li, D.; Zhang, Z.; Zhang, H.; Wang, Y. *Org. Lett.* **2014**, *16*, 880−883.

(5) Araneda, J. F.; Piers, W. E.; Heyne, B.; Parvez, M.; McDonald, R. *Angew. Chem., Int. Ed.* **2011**, *50*, 12214−12217.

(6) Nawn, G.; Oakley, S. R.; Majewski, M. B.; McDonald, R.; Patrick, B. O.; Hicks, R. G. *Chem. Sci.* **2013**, *4*, 612−621.

(7) Yoshii, R.; Suenaga, K.; Tanaka, K.; Chujo, Y. *Chem. - Eur. J.* **2015**, *21*, 7231−7237.

(8) (a) Wakamiya, A.; Taniguchi, T.; Yamaguchi, S. *Angew. Chem., Int. Ed.* **2006**, *45*, 3170−3173. (b) Liu, Q. D.; Mudadu, M. S.; Thummel, R.; Tao, Y.; Wang, S. *Adv. Funct. Mater.* **2005**, *15*, 143−154.

(9) (a) Tamgho, I.-S.; Hasheminasab, A.; Engle, J. T.; Nemykin, V. N.; Ziegler, C. J. *J. Am. Chem. Soc.* **2014**, *136*, 5623−5626. (b) Zhang, H.; Hong, X.; Ba, X.; Yu, B.; Wen, X.; Wang, S.; Wang, X.; Liu, L.; Xiao, J. *Asian J. Org. Chem.* **2014**, *3*, 1168−1172. (c) Curiel, D.; Más-Montoya, M.; Usea, L.; Espinosa, A.; Orenes, R. A.; Molina, P. *Org. Lett.* **2012**, *14*, 3360−3363.

(10) (a) Wei, J.; Han, B.; Guo, Q.; Shi, X.; Wang, W.; Wei, N. *Angew. Chem., Int. Ed.* **2010**, *49*, 8209−8213. (b) Chen, L.; Puniredd, S. R.; Tan, Y.-Z.; Baumgarten, M.; Zschieschang, U.; Enkelmann, V.; Pisula, W.; Feng, X.; Klauk, H.; Müllen, K. *J. Am. Chem. Soc.* **2012**, *134*, 17869−17872. (c) Li, X.; Zhu, Y.; Shao, J.; Wang, B.; Zhang, S.; Shao, Y.; Jin, X.; Yao, X.; Fang, R.; Shao, X. *Angew. Chem., Int. Ed.* **2014**, *53*, 535−538. (d) Wang, X.-Y.; Zhuang, F.-D.; Wang, X.-C.; Cao, X.-Y.; Wang, J.-Y.; Pei, J. *Chem. Commun.* **2015**, *51*, 4368−4371.

(11) Bertrand, H.; Granzhan, A.; Monchaud, D.; Saettel, N.; Guillot, R.; Clifford, S.; Guédin, A.; Mergny, J.-L.; Teulade-Fichou, M.-P. *Chem. - Eur. J.* **2011**, *17*, 4529−4539.

(12) Wang, X.; Zhang, F.; Liu, J.; Tang, R.; Fu, Y.; Wu, D.; Xu, Q.; Zhuang, X.; He, G.; Feng, X. *Org. Lett.* **2013**, *15*, 5714−5717.

(13) Yang, Y.; Su, X.; Carroll, C. N.; Aprahamian, I. *Chem. Sci.* **2012**, *3*, 610−613.

(14) Gong, S.; Liu, Q.; Wang, X.; Xia, B.; Liu, Z.; He, W. *Dalton Trans.* **2015**, *44*, 14063−14070.

(15) (a) Woo, H.; Cho, S.; Han, Y.; Chae, W.-S.; Ahn, D.-R.; You, Y.; Nam, W. *J. Am. Chem. Soc.* **2013**, *135*, 4771−4787. (b) Kubota, Y.; Hara, H.; Tanaka, S.; Funabiki, K.; Matsui, M. *Org. Lett.* **2011**, *13*, 6544−6547.

(16) (a) Wu, Y.; Lu, H.; Wang, S.; Li, Z.; Shen, Z. *J. Mater. Chem. C* **2015**, *3*, 12281−12289. (b) Glotzbach, C.; Godeke, N.; Frohlich, R.; Daniliuc, C.-G.; Saito, S.; Yamaguchi, S.; Wurthwein, E.-U. *Dalton Trans.* **2015**, *44*, 9659−9671.

(17) Bhongale, C. J.; Chang, C.-W.; Lee, C.-S.; Diau, E. W.-G.; Hsu, C.-S. *J. Phys. Chem. B* **2005**, *109*, 13472−13482.

(18) (a) Dou, C.; Ding, Z.; Zhang, Z.; Xie, Z.; Liu, J.; Wang, L. *Angew. Chem., Int. Ed.* **2015**, *54*, 3648−3652. (b) Dou, C.; Long, X.; Ding, Z.; Xie, Z.; Liu, J.; Wang, L. *Angew. Chem., Int. Ed.* **2016**, *55*, 1436−1440.

DOI: 10.1021/acs.orglett.6b00335
Org. Lett. 2016, 18, 1398−1401